

Multi-objective Evolution of Drone Morphology

Elijah H. W. Ang¹, Christophe De Wagter¹ and Guido C. H. E. de Croon¹

Abstract—The design of multicopter drones has remained almost the same since its inception. While conventional designs, such as the quadcopter, work well in many cases, they may not be optimal in specific environments or missions. This paper revisits rotary drone design by exploring which body morphologies are optimal for different objectives and constraints. Specifically, an evolutionary algorithm is used to produce optimal drone morphologies for three objectives: (1) high thrust-to-weight ratio, (2) high maneuverability, and (3) small size. To generate a range of optimal drones with performance trade-offs between them, the non-dominated sorting genetic algorithm II, or NSGA-II is used. A randomly sampled population of 600 is evolved over 2000 generations. The NSGA-II algorithm evolved drone bodies that outperform a standard 5-inch 220 mm wheelbase quadcopter in at least one of the three objectives. The three extrema in the Pareto front show improvement of 487.8%, 23.5% and 4.8% in maneuverability, thrust-to-weight ratio and size, respectively. The improvement in maneuverability can be attributed to the tilt angles of the propellers, while the increase in thrust-to-weight ratio is primarily due to the higher number of propellers. The quadcopter is located on the Pareto front for the three objectives. However, our results also show that other designs can be better depending on the objectives.

Index Terms—Aerial robotics, Drone morphology, Evolution, Multi-objective optimization, Pareto front

I. INTRODUCTION

In recent years, multicopter drones have been widely adopted for various applications, such as surveillance, site inspection and disaster response [1]. Since its inception, drones have always adopted the same simple and conventional designs. An example of this is the standard quadcopter. The advantages of these designs are that they have been researched and developed extensively, they are simple to construct, and the implementation of controls is intuitive [2], [3]. While such drones may perform adequately for a wide range of applications, they may not be the most optimal design for specific use cases.

Nature and biology have proven that the morphology varies wildly across species [4]. The morphology of each species has been adapted and optimized to produce the best performance needed for its specific environmental niche. This optimization is performed via the natural selection process where the best-performing individuals are given the opportunity to reproduce and pass on their genes to the next generation, while the worst-performing individuals get eliminated [5]. This process occurs over multiple generations before an optimal morphology is achieved.

All authors are with Faculty of Aerospace Engineering, Delft University of Technology, 2629 HS Delft, The Netherlands. (email: e.h.w.ang@tudelft.nl; c.dewagter@tudelft.nl; g.c.h.e.deCroon@tudelft.nl)

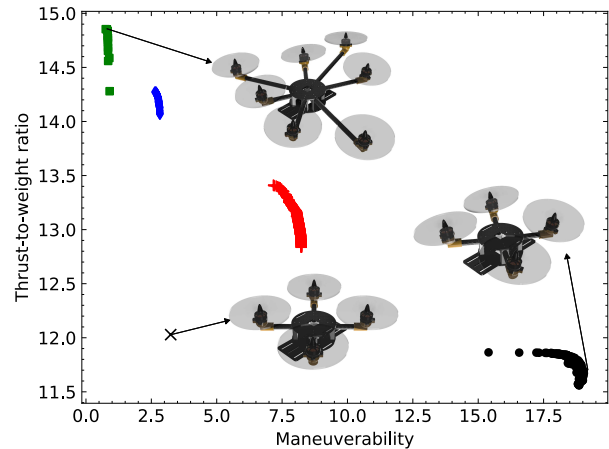


Fig. 1. We use multi-objective optimization to generate novel propeller-based drone designs. Here the Pareto front is shown for two of the studied objectives, thrust-to-weight ratio and maneuverability, with renders of a standard quadcopter (indicated with the cross, \times), drone with the highest thrust-to-weight ratio (green squares on the top left) and drone with highest maneuverability (black dots on the bottom right).

Drawing inspiration from nature, the designs of various systems can also be optimized via the same evolutionary process. This method has proven to be successful in various systems such as antenna design [6], walking robots [7], modular robots [8] and recently on winged aircraft [9].

In this paper, we explore whether an artificial evolution process can improve upon the design of the most occurring drone type: the multicopter. Specifically, a multi-objective approach to evolve drone morphology is presented. The non-dominated sorting genetic algorithm II (NSGA-II) is used for the evolution of drone bodies. To ensure that the drones produced from the evolutionary algorithm are physically viable, their fitness will be evaluated using model-based objective functions, such as hovering capabilities, maneuverability, thrust-to-weight ratio and size. The main contributions of this paper are (1) an efficient model-based fitness evaluation for the evolution of drones, (2) the evolution of drone morphology with guaranteed viability and (3) multi-objective evolution which produces a diverse range of optimal drones. The rest of the paper is organized as follows. Section II looks into related work found in the literature. Section III presents model-based objective functions for drones with arbitrary configurations. Section IV describes the evolution process as well as the genotype to phenotype mapping. Section V discusses the results obtained from evolving drone bodies. Lastly, Section VI concludes this paper.

II. RELATED WORK

Designing and optimizing systems are often expensive, time consuming and require significant domain knowledge. As such, several researchers have drawn inspiration from nature by adopting evolutionary processes to optimize their systems. Hornby et al. [6] proposed a novel antenna designed using an evolutionary algorithm that performs better than human-designed antennas. Vujovic et al. [7] combined evolution with development stages for the evolution of real-world walking robots. The development stage simulates the growing process from infancy to adulthood for each species.

When it comes to drones, evolutionary algorithms have been successful in optimizing the controller, or the "brain", of the drones. For instance, Shamshirgaran et al. [10] performed multi-objective evolution using particle swarm optimization (PSO) and biogeography-based optimization (BBO) to tune the parameters of a PD controller for a quadcopter. Similarly, Yazid et al. [11] used evolutionary algorithms such as genetic algorithm (GA), PSO and artificial bee colony (ABC) to tune a Takagi-Sugeno-Kang fuzzy logic controller for position control of a quadcopter. Additionally, the optimization of drone bodies has been investigated in the literature. Du et al. [12] produced an optimized multicopter from an initial user design using convex optimization algorithms. Their algorithm took user-provided designs such as the quadcopter and pentacopter and modified the geometry for increased flight time and payload, respectively. Similarly, Carlone and Pinciroli [13] co-designed drone bodies and hardware using linear programming methods. Their algorithm selects the best components, such as actuators and sensors, to meet specific objectives and constraints. On the other hand, Bergonti et al. [9] optimized the topology and control of morphing wing drones using an evolutionary algorithm. Their simulation results showed that the evolved morphing wing drone outperforms a standard fixed-wing aircraft in terms of energy efficiency and mission time.

While optimization of drone bodies has been investigated in the past, the most common methods involve linear and non-linear programming, while evolutionary algorithms are seldom explored. Additionally, much of the past research optimized a single objective function at a time, which restricted the diversity of drone designs. In our work, we provide an evolution-based morphology optimization of multicopters with multiple degrees of freedom. We also consider multiple objectives, with the aim of generating a diverse range of drone designs that excels in various scenarios while achieving more significant advances over the common quadcopter design.

III. MODEL-BASED OBJECTIVE FUNCTIONS

To automatically optimize drone designs, we need to model their dynamics. In this section, we explain how we model the drones in order to calculate each design's performance in terms of the three optimization objectives.

A. Actuator Effectiveness Matrices

The thrust and moment produced by a rotor and propeller are directly proportional to the square of the rotational speed of the propeller, and are given as,

$$\begin{aligned} F &= k_f \omega^2 \\ M &= k_m \omega^2 \end{aligned} \quad (1)$$

where ω is the rotation speed of the propeller, and k_f and k_m are the thrust and moment coefficients of the propeller, respectively. It is convenient to define an actuator command $\eta \in [0, 1]$ which maps linearly to $[0, \omega_{max}^2]$ in order to linearize the equations. By combining the effects of all propellers, the forces and moments acting about the C.G. of the drone can be condensed into a single matrix equation. For a drone with n propellers, the specific forces and moments are defined as,

$$\begin{aligned} \mathbf{f} &= \mathbf{B}_f \eta \\ \boldsymbol{\tau} &= \mathbf{B}_m \eta \end{aligned} \quad (2)$$

where $\eta \in \mathbb{R}^n$ is the vector of actuator commands, $\mathbf{f} \in \mathbb{R}^3$ and $\boldsymbol{\tau} \in \mathbb{R}^3$ are the specific force and moment vectors, respectively, and $\mathbf{B}_f \in \mathbb{R}^{3 \times n}$ and $\mathbf{B}_m \in \mathbb{R}^{3 \times n}$ are the force and moment actuator effectiveness matrices, respectively. These matrices are a function of the positions and orientations of the propellers, as well as the inertia properties of the entire drone.

B. Static Hovering

In order to hover, the drones must produce sufficient thrust to overcome their weight and maintain their attitude. Allowing drones with arbitrary configuration may result in multiple hovering attitudes. Hence, the aim is to find an optimized set of control inputs $\hat{\eta}$ from control space $\eta \in \mathbb{R}^n$ which allows the drone to hover statically at minimum cost. If a solution cannot be found, the drone is unable to hover statically. This can be defined as a non-linear programming problem as follows,

$$\begin{aligned} \min \quad & J = \hat{\eta}^T \hat{\eta} \\ \text{s.t.} \quad & \|\mathbf{B}_f \hat{\eta}\|_2 = g \\ & \mathbf{B}_m \hat{\eta} = \mathbf{0} \\ & \underline{\eta} \leq \hat{\eta} \leq \bar{\eta}. \end{aligned} \quad (3)$$

where g is the gravitational acceleration, $\underline{\eta}$ is the lower actuation limit and $\bar{\eta}$ is the upper actuation limit. The first constraint specifies that the optimal control input has to produce enough thrust to overcome gravity in order to hover. The second constraint states that the optimal control input has to result in zero resultant moments acting on the body of the drone while hovering. The final equation ensures that the control inputs are kept between the upper and lower actuation limits. The sequential least-squares programming (SLSQP) algorithm is used to find the optimal control inputs.

C. Non-static Hovering

In some configurations, the drones may not be able to hover statically without rotating. Instead, these drones can maintain their position while spinning about their yaw axis. A clear example of this is a tricopter without a tilting tail rotor. While it is not optimal, such designs should not be discarded as they may still contain desirable properties, such as the ability to hold their altitude, which may be carried over to the next generation of drones during evolution. Hence, a set of control inputs $\hat{\eta}$ from control space $\eta \in \mathbb{R}^n$ which allows the drone to hover while spinning at minimum cost can be computed using the following constraints,

$$\begin{aligned} \min \quad & J = \hat{\eta}^T \hat{\eta} \\ \text{s.t.} \quad & \|\mathbf{B}_f \hat{\eta}\|_2 = g \\ & \|\mathbf{B}_f \hat{\eta} \times \mathbf{B}_m \hat{\eta}\|_2 = 0 \\ & \underline{\eta} \leq \hat{\eta} \leq \bar{\eta} \end{aligned} \quad (4)$$

The first and the last constraints are the same as for static hovering. The second constraint no longer requires zero resultant moment acting on the body. Instead, it requires that the direction of thrust and the axis of rotation are parallel, resulting in a drone that spins while hovering. This is done by ensuring that the magnitude of the cross product between the thrust and moment vectors has a magnitude of zero.

D. Thrust-to-weight Ratio

The thrust-to-weight ratio is used as a proxy for several secondary goals at once. With a higher thrust-to-weight ratio, the drone can either fly faster or carry larger batteries for more flight time, carry more payload for better mission results or carry better sensors and processing. These all lead to improved mission performance which forms a secondary optimization goal. Once $\hat{\eta}$ has been computed, the maximum possible thrust-to-weight ratio can be computed by scaling the control inputs until control input saturation is reached for at least one of the propellers. Since the control inputs are scaled to a range of $[0, 1]$, this can be computed using,

$$\hat{\eta}_{max} = \frac{\hat{\eta}}{\max_i \hat{\eta}_i} \quad (5)$$

where $\hat{\eta}_{max}$ gives the control input which results in largest thrust-to-weight ratio without exceeding the upper or lower bounds and $\hat{\eta}_i$ gives the i th control input. Hence, the thrust-to-weight ratio is given as,

$$\alpha = \frac{\|\mathbf{B}_f \hat{\eta}_{max}\|_2}{g} \quad (6)$$

where α is the thrust-to-weight ratio.

E. Controllability and Maneuverability

The controllability determines if a drone has full moment actuation. Typically, a drone is controllable if the controllability matrix has full row rank. However, this measure does not provide a measure of the agility or maneuverability of the drone. Instead, a better indicator can be obtained by using

the controllability Gramian. For the dynamics given by Eq. 2, the Gramian is computed as,

$$\mathbf{W}_c = \mathbf{B}_m \mathbf{B}_m^T \quad (7)$$

where $\mathbf{W}_c \in \mathbb{R}^{3 \times 3}$ gives the controllability Gramian [14]. The eigenvalues of the Gramian give an indication on the maneuverability of each of the principal axes defined by their corresponding eigenvectors. With higher maneuverability, drones will be able to perform aggressive maneuvers, which is useful in applications such as drone racing or physically interacting with the world. As a more agile drone is desired, the maneuverability of the drone will be characterized by the smallest eigenvalue, which corresponds to its least maneuverable principal axis, given as,

$$\lambda = \min \text{eig}(\mathbf{W}_c). \quad (8)$$

F. Size of Drone

Generally, smaller drones are preferred as they will be able to navigate and squeeze through small spaces. However, the trade-off is that a smaller drone may not have the space to accommodate heavier equipment such as high-resolution cameras or GPU-enabled companion computers. The size of a drone can be parameterized using the volume of its convex hull formed by the propeller positions. In 2D cases where propellers are placed on the same plane, the area of the convex hull will be used instead.

IV. EVOLUTION OF DRONE BODIES

A. Phenotype and Genotype

The phenotype of the drone defines the location and direction of the propellers. In this study, the parameters of the drones to be evolved are given as follows:

- 1) number of propellers: $n \in \{4, 5, 6, 7, 8\}$
- 2) arm length: $l \in [0.1 \text{ m}, 0.3 \text{ m}]$
- 3) arm angle: $\theta \in [-180^\circ, 180^\circ]$
- 4) propeller inclination: $\varphi \in [0^\circ, 15^\circ]$
- 5) propeller azimuth wrt. arm: $\psi \in [-90^\circ, 90^\circ]$
- 6) propeller direction: $R \in \{\text{'CCW'}, \text{'CW'}\}$

In this study, for manufacturability purposes, we use the constraint that all motors are placed on the $x-y$ plane of the drone. The minimum number of propellers is 4 as that is the minimal condition required for a drone to achieve basic actuation [15]. The flight controller stack is kept at 250 g, which is based on the weight of a rectangular 4s, 2200 mAh lipo battery. The longitudinal axis of the battery is oriented parallel to the x axis of the drone. 5-inch propellers are used in all cases.

The genotype is a direct representation of the phenotype and can be broken down into eight subsections, one for each propeller. A visual representation of the genotype is shown in Figure 2. Each value in the subsection is within the range of $[-1, 1]$, and is directly mapped to the parameters defined above. Continuous parameters (parameters 2 to 5) are linearly mapped while discrete parameters (parameters 1 and 6) are first discretized evenly before mapping. To keep the genotype

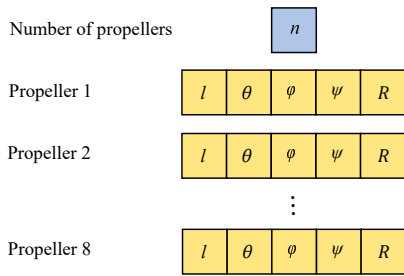


Fig. 2. Illustration of genotype used for evolution.

length the same while varying the number of propellers, only the first n subsections are mapped into propellers in the phenotype. The remaining subsections stay in the genotype and act as "phantom" propellers which have a chance of being activated during the evolution process. In the event that propellers intersect each other, all arm lengths will scale up until sufficient distance between propellers is achieved. As a result, the arm length may exceed the upper limit of 0.3 m as originally prescribed in the phenotype mapping. It is important to note that this scaling is part of the genotype-to-phenotype mapping process, and the genotype remains the same after scaling.

B. NSGA-II and Fitness Evaluation

The initial population of genotypes is generated using the Latin hypercube sampling method to ensure distributed sampling across the solution space. The evolution of the drones is performed using the NSGA-II algorithm, which is an elitist multi-objective evolutionary algorithm that ranks individuals based on non-dominated sort [16].

As NSGA-II is a multi-objective optimization algorithm, the fitness function is not determined by a single metric. Instead, multiple objective functions are computed and individuals are ranked by the number of individuals that dominate it. Hence, individuals who get dominated the least will be ranked the highest, producing a range of Pareto optimal results. Subsequent rankings will result in their own Pareto front. NSGA-II is used as it provides a fast algorithm for the non-dominated sort as well as solution density estimation to preserve diversity within the population. Assuming that the drones limited by the phenotype can accommodate heavier onboard equipment, the objective functions in this experiment are to maximize thrust-to-weight ratio and maneuverability while minimizing the volume of the bounding box of the drone. Additionally, drones with the ability to hover statically are ranked ahead of drones that can only achieve spinning hover, which is in turn ranked ahead of drones that cannot hover.

V. RESULTS AND DISCUSSIONS

An initial population of size 600 evolved over 2000 generations using NSGA-II. A value-wise arithmetic crossover scheme with a 20% mutation rate is used to populate the next generation in the evolutionary process. Parents are selected using the binary tournament selection algorithm. Simulation

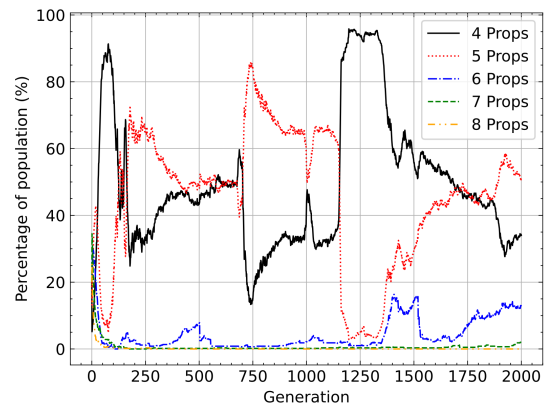


Fig. 3. Percentage of number of arms for each generation.

results obtained from the evolution process are compared with a standard 5-inch quadcopter with 220 mm wheelbase.

A. Evolution History

Figure 3 shows the proportion of drones with varying numbers of propellers across the generations. The initial random population starts with approximately 20% of each propeller number. However, as the evolution progresses, the number of 8-propeller drones quickly diminishes. As a result, the remaining drones have between 4 to 7 propellers, with the 5 propeller drones making up more than half of the population. It is observed that for the majority of the generations after 150, drones with 7 propellers are fully eliminated. However, due to the mutation process, 7 propeller drones start to reappear and survive the evolution process, and make up 2% of the population. On the other hand, 8 propeller drones are unable to benefit from mutation.

B. Pareto Optimal Drones

Figures 4, 5 and 6 show the optimal Pareto front at the end of evolution projected on the $\lambda - \alpha$, $\lambda - \text{size}$ and $\text{size} - \alpha$ planes, respectively. Looking at the plots, size, maneuverability and thrust-to-weight ratio are very clearly clustered according to the number of propellers, making it a key parameter determining the drone's characteristics. Drawing comparisons to nature, each cluster acts as a distinct species where each individual within a species tends to have similar characteristics. Figures 7 and 8 show the drone with the highest thrust-to-weight ratio and the smallest drone with the highest maneuverability, respectively.

Generally, increasing the number of propellers leads to an increase in size and thrust-to-weight ratio with a reduction in maneuverability. Decreasing the size leads to an increase in maneuverability, which are both desirable according to the objectives. On the other hand, an increase in the thrust-to-weight ratio leads to an increase in size as well as a decrease in maneuverability. This shows that it is impossible to maximize all three objectives at once, and presents a trade-off between size, thrust-to-weight ratio and maneuverability for the optimal drones.

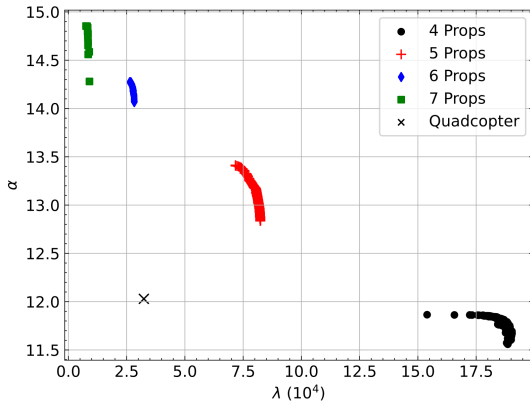


Fig. 4. Scatter plot of Pareto optimal drones' thrust-to-weight ratio against maneuverability at generation 2000.

Comparing the results with the standard quadcopter, the evolution process managed to obtain drones that outperform the quadcopter in each of the three objectives. The drone with the highest α presents an improvement of 23.5% to the thrust-to-weight ratio while the most maneuverable drone shows a significant increase in maneuverability by 487.8%. The increase in thrust-to-weight ratio is largely due to the use of additional propellers while the increase in maneuverability can be attributed to tilted propellers and smaller drones for increased specific moments, especially about the yaw axis. The reduction in size for the smallest drone is 4.8%, which is small compared to the improvement in thrust-to-weight ratio and maneuverability. Drones with high maneuverability will be beneficial in situations where fast and tight maneuvers are required, such as in drone racing. On the other hand, having a high thrust-to-weight ratio is necessary for performing tasks such as navigation or simultaneous localization and mapping (SLAM) with heavy equipment such as depth cameras and powerful onboard computers. Lastly, small drones are generally preferred when needed to navigate through dense and cluttered environments such as unmanned forests. While the evolved drones manage to dominate the quadcopter in Figures 4 and 5, the evolution process is unable to obtain drones that are smaller yet process higher thrust-to-weight ratio than a standard quadcopter. In this regard, the standard quadcopter remains to be one of the non-dominated optimal designs.

C. Discussion

As seen from the results in Figure 3, drones with 8 propellers are eliminated by the end of the evolution process, despite having equal proportions of 4 to 8 propeller drones at the beginning. Larger drones generally result in lower maneuverability, as shown in Figure 5. The angular acceleration due to a single propeller can be modeled as,

$$\dot{\Omega} \propto \frac{l}{ml^2 + \frac{\mu}{3}l^3 + I_{fc}} \quad (9)$$

where $\dot{\Omega}$ gives the angular acceleration, l gives the length of the arm, m is the mass of the motor for the propeller,

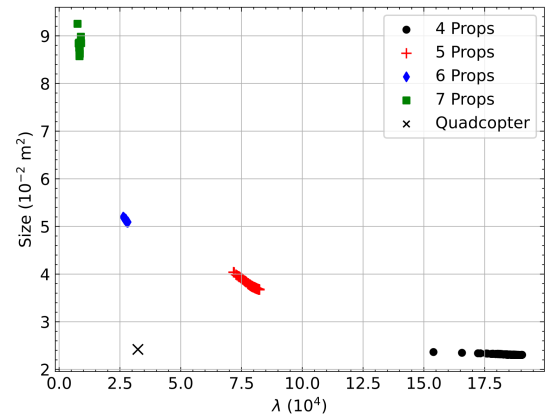


Fig. 5. Scatter plot of Pareto optimal drones' size against maneuverability at generation 2000.

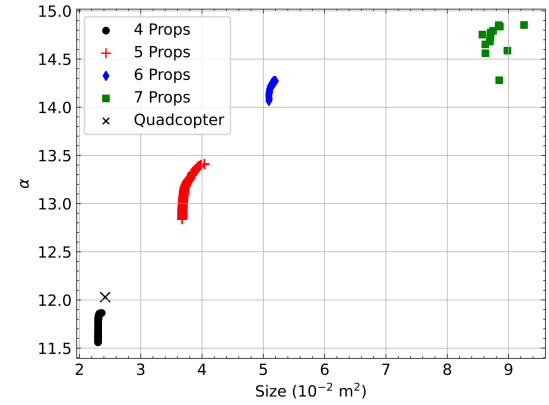


Fig. 6. Scatter plot of Pareto optimal drones' thrust-to-weight ratio against size at generation 2000.

μ is the mass per unit length of the arm connecting the motor to the body, and I_{fc} is the moment of inertia due to the battery and flight controller stack. The numerator represents the moments produced while the denominator represents the moment of inertia of the system. While the moment generated by the propeller increases linearly with the length of the arm, the resulting moment of inertia increases quadratically with the length, which results in an overall reduction in the angular acceleration. Moreover, propellers placed further apart require longer arms which further add to the mass and moment of inertia of the drone, which is represented by a cubic relationship. The angular acceleration given by Eq. 9 increases to a maximum value within a very narrow band of l which lies outside of the phenotype mapping range before decreasing with further increase of the arm length. As a result, the most maneuverable drone is also the smallest drone after evolution, as shown in Figure 8.

On the other hand, larger drones tend to have a higher thrust-to-weight ratio. Generally, having more propellers will result in a higher thrust-to-weight ratio, which also requires the drones to be larger to prevent propellers from intersecting each other. Despite this, only a few 7 or 8-propeller drones emerged from the evolution process. Apart from having a

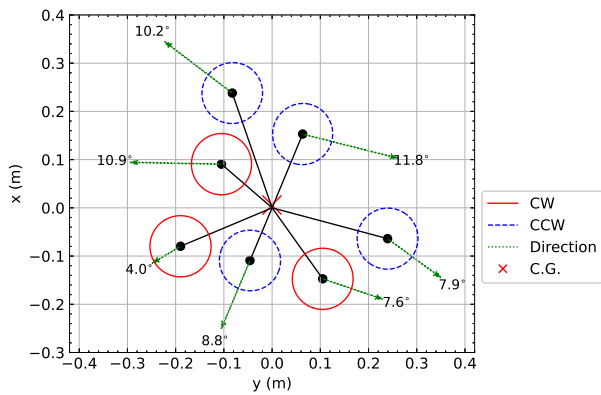


Fig. 7. Drone with highest thrust-to-weight ratio after generation 2000.

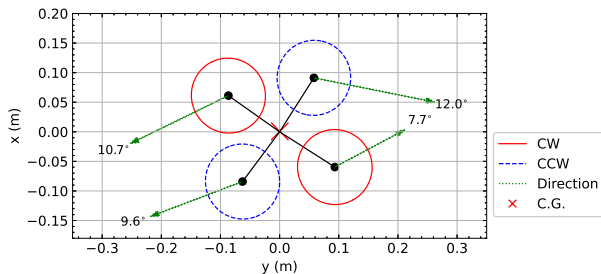


Fig. 8. Smallest and most maneuverable drone after generation 2000.

high number of propellers, the propellers need to be evenly spaced apart and evenly actuated to achieve a high thrust-to-weight ratio. In cases where the propellers are not evenly spaced apart, some propellers may require higher actuation to counter the moments from other propellers while hovering, which will result in earlier saturation of these propellers. In such cases, the maximum possible thrust-to-weight ratio is reduced.

The evolutionary process is unable to obtain the drone with the theoretically highest thrust-to-weight ratio, which is an octocopter with all propellers pointing vertically up, spaced evenly apart. This is because the viable and optimal solution space for 8-propeller drones is very small as compared to drones with fewer propellers. This results in difficulty in the search for optimal drones with 8 propellers despite having a high mutation rate of 20% for exploration, resulting in them getting eliminated from the population very early on.

While the evolutionary process is effective in obtaining drones that outperform a standard quadcopter in at least one objective, it was unable to fully dominate the quadcopter. The design of the standard quadcopter has arms positioned at equal distances from each other, which allows for shorter arms to be used without the propellers impeding each other. At the same time, the propellers are all pointing vertically upwards. The combination of these two results in a sufficiently small drone with the highest thrust-to-weight ratio possible for a 4-propeller drone. However, this leads to yaw maneuverability being a major weakness of a quadcopter as the only source of actuation is from the counter-torque produced from spinning the propeller.

Currently, the results from the evolution are evaluated in simulation, with the manufacturing and flight tests of prototypes to be performed as part of our future work. Slight differences in performance are expected as the experiments are performed in real life. These deviations will primarily be due to the precision required in the manufacturing process. However, since the objectives and performance metrics are developed using the physics of drones, we expect the real-world designs to achieve similar performance gains as the evolved drones.

VI. CONCLUSIONS

In this paper, multi-objective optimization of drone bodies is performed using the NSGA-II algorithm to maximize the thrust-to-weight ratio and maneuverability while minimizing its size. The NSGA-II algorithm generated a range of drone bodies that can outperform a standard quadcopter in at least one of the three objectives, with the smallest drone being 4.8% smaller, and the most maneuverable and highest thrust-to-weight ratio being 487.8% and 23.5% better than a standard quadcopter, respectively. The Pareto front provides insights into the performance trade-offs when modifying the morphology of the drones. Generally, drones with more propellers can generate a higher thrust-to-weight ratio at a cost of larger size and lower maneuverability. On the other hand, possessing fewer propellers results in smaller and more maneuverable drones at the cost of a lower thrust-to-weight ratio. At the same time, tilting the propellers generally improves the maneuverability of the drone by increasing control authority in the yaw axis. Results show that the standard quadcopter remains on the Pareto front. However, depending on the required objectives, other drone designs have been shown to possess better performance.

Manufacturing and flight tests of the drones will be performed to determine the improvement in performance in real life, and this will be investigated as part of our future work. While we foresee some reality gap, similar performance gains from the evolved drones can be expected as the objectives and performance metrics are derived from well-studied drone physics.

ACKNOWLEDGMENT

This work was supported by the European Commission Horizon project SPEAR under grant agreement 101119774.

REFERENCES

- [1] M. Hassanalain and A. Abdelkefi, "Classifications, applications, and design challenges of drones: A review," *Progress in Aerospace sciences*, vol. 91, pp. 99–131, 2017.
- [2] D. BBVL and P. Singh, "A survey on design and development of an unmanned aerial vehicle (quadcopter)," *International Journal of Intelligent Unmanned Systems*, vol. 4, no. 2, pp. 70–106, 2016.
- [3] J. Paredes, P. Sharma, B. Ha, M. Lanchares, E. Atkins, P. Gaskell, and I. Kolmanovsky, "Development, implementation, and experimental outdoor evaluation of quadcopter controllers for computationally limited embedded systems," *Annual Reviews in Control*, vol. 52, pp. 372–389, 2021.
- [4] H. H. Lund, J. Hallam, and W.-P. Lee, "Evolving robot morphology," in *Proceedings of 1997 IEEE International Conference on Evolutionary Computation (ICEC'97)*. IEEE, 1997, pp. 197–202.

- [5] S. Forrest, "Genetic algorithms: principles of natural selection applied to computation," *Science*, vol. 261, no. 5123, pp. 872–878, 1993.
- [6] G. S. Hornby, J. D. Lohn, and D. S. Linden, "Computer-automated evolution of an X-band antenna for NASA's space technology 5 mission," *Evolutionary computation*, vol. 19, no. 1, pp. 1–23, 2011.
- [7] V. Vujovic, A. Rosendo, L. Brodbeck, and F. Iida, "Evolutionary developmental robotics: Improving morphology and control of physical robots," *Artificial life*, vol. 23, no. 2, pp. 169–185, 2017.
- [8] J. Külz and M. Althoff, "Optimizing modular robot composition: A lexicographic genetic algorithm approach," in *2024 IEEE International Conference on Robotics and Automation (ICRA)*. IEEE, 2024, pp. 16 752–16 758.
- [9] F. Bergonti, G. Nava, V. Wüest, A. Paolino, G. L'Erario, D. Pucci, and D. Floreano, "Co-design optimisation of morphing topology and control of winged drones," in *2024 IEEE International Conference on Robotics and Automation (ICRA)*. IEEE, 2024, pp. 8679–8685.
- [10] A. Shamsirgaran, H. Javidi, and D. Simon, "Evolutionary algorithms for multi-objective optimization of drone controller parameters," in *2021 IEEE Conference on Control Technology and Applications (CCTA)*. IEEE, 2021, pp. 1049–1055.
- [11] E. Yazid, M. Garratt, and F. Santoso, "Position control of a quadcopter drone using evolutionary algorithms-based self-tuning for first-order Takagi–Sugeno–Kang fuzzy logic autopilots," *Applied Soft Computing*, vol. 78, pp. 373–392, 2019.
- [12] T. Du, A. Schulz, B. Zhu, B. Bickel, and W. Matusik, "Computational multicopter design," *ACM Transactions on Graphics*, 2016.
- [13] L. Carlone and C. Pinciroli, "Robot co-design: beyond the monotone case," in *2019 International Conference on Robotics and Automation (ICRA)*. IEEE, 2019, pp. 3024–3030.
- [14] S. L. Brunton and J. N. Kutz, *Data-driven science and engineering: Machine learning, dynamical systems, and control*. Cambridge University Press, 2022.
- [15] M. Hamandi, F. Usai, Q. Sablé, N. Staub, M. Tognon, and A. Franchi, "Design of multirotor aerial vehicles: A taxonomy based on input allocation," *The International Journal of Robotics Research*, vol. 40, no. 8-9, pp. 1015–1044, 2021.
- [16] K. Deb, A. Pratap, S. Agarwal, and T. Meyarivan, "A fast and elitist multiobjective genetic algorithm: NSGA-II," *IEEE transactions on evolutionary computation*, vol. 6, no. 2, pp. 182–197, 2002.